Chapter 3

A Problem in Petroleum Reservoir Simulation

Alistair Fitt[1], Brian Seymour[2], John Stockie[3], Michèle Titcombe[4], Tony Ware[5]

Report compiled by Brian Seymour

3.1 Introduction

This report describes the results of the analysis of a problem in petroleum reservoir simulation presented by Peter Sammon of the Computer Modeling Group Ltd. (CMG). A summary of the problem, including contact information, is in the introductory pages of these proceedings.

The flow of two fluids (here, oil and water) in an underground petroleum reservoir is typically modeled by two partial differential equations: a parabolic equation for the fluid pressure in the reservoir, and a non-linear hyperbolic conservation law describing the fluid movement. In general, these equations are coupled through their coefficients, and are invariably solved numerically using finite difference schemes. The major difficulty in using these schemes is that they are very sensitive to the orientation of the finite difference grid.

The problem posed by Peter Sammon was to find an exact solution to the equations governing two-phase petroleum reservoirs that could be used to validate the numerical code used by the Computer Modeling Group in its simulations. Ideally, the analysis would result in an exact solution to the coupled system of equations for a specific rectangular geometry. It was soon realized that this was a hopeless task, so the group set out to find compromises that would still provide useful validation examples.

3.2 The Physical Problem

A simple model of the physical problem consists of a horizontal section of the petroleum reservoir in which water is pumped into an injector (source) at a specified velocity and oil extracted from a producer (sink) at a remote site. The geometry of the region shown in Figure 3.1 is typically part of a much larger region with many sources and sinks.

The saturation of water S is

$$S = \begin{cases} 1 & \text{if all water,} \\ 0 & \text{if all oil.} \end{cases} \tag{2.1}$$

[1]Faculty of Mathematical Studies, University of Southampton
[2]Department of Mathematics, University of British Columbia
[3]Department of Mathematics, Simon Fraser University
[4]Department of Mathematics, University of British Columbia
[5]Clinical Neurosciences, University of Calgary

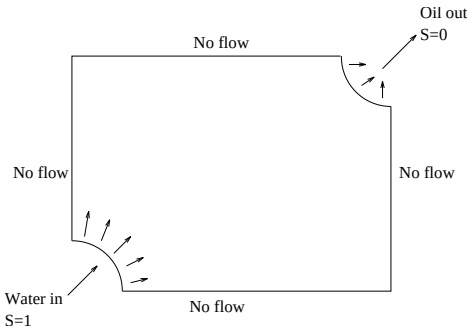

Figure 3.1: Typical reservoir simulation geometry.

3.3 Potential Problems

While there are conflicting opinions regarding the details of the model equations (e.g. a three-phase model), whichever model is used, the flow equations must be solved numerically, typically using upwind differencing. The major difficulty with this approach is that the numerical solutions exhibit grid orientation dependency. On grids such as those shown in Figure 3.2, the numerical scheme will give different (sometimes *very* different) results for the same problem. McCracken et al. [3] examine

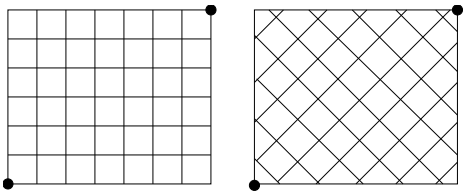

Figure 3.2: Rectangular grid orientations.

a numerical method for eliminating the dependence of the solution on grid orientation.

A question one might ask is whether or not the numerical scheme becomes more accurate as the grid size decreases? (See Section 3.8 for further comments regarding the well-posedness of the problem.)

3.4 Model Equations

The simplest 2-D model of petroleum reservoir simulation is described by the equations

$$\nabla \cdot (\lambda(S)\nabla p) = 0, \text{and } \phi S_t = \nabla \cdot (f(S)\lambda(S)\nabla p), \tag{4.2}$$

where p is the pressure, S the saturation and ϕ the porosity of the rock. The **total mobility**, $\lambda(S)$, and **fractional flow**, $f(S)$, are the key functions that determine the different forms of solutions.

The total mobility function is typically of the form:

$$\lambda(S) = \frac{k}{\mu_w}\left(\frac{(1-S)^\beta}{M} + S^\alpha\right), \tag{4.3}$$

where μ_w is the viscosity of water and k is the permeability of the rock. Similarly the fractional flow function is

$$f(S) = \frac{S^\alpha}{S^\alpha + \dfrac{(1-S)^\beta}{M}}, \tag{4.4}$$

where α and β are constants such that $\alpha \geqslant 1$ and $\beta \geqslant 1$. In these functions the **mobility** M is defined as

$$M = \frac{\mu_o}{\mu_w}, \tag{4.5}$$

and typically $M > 1$. For simplicity we take ϕ and k as constants.

Figure 3.3 shows the dependence of key functions on the constants M, α and β.

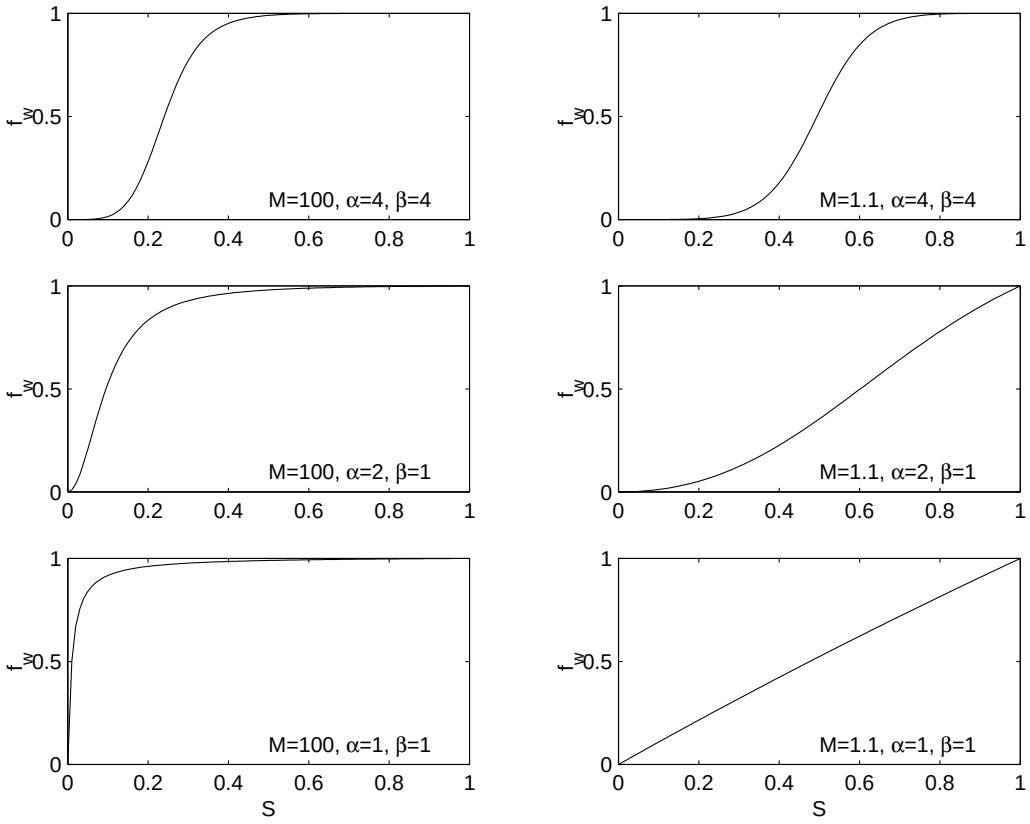

Figure 3.3: Dependence of key functions on M, α, and β.

3.5 Approaches for Finding Exact Solutions

Several approaches were initially considered:

[1] Two simple special solutions:

(a) Traveling waves of the form $S = S(ax + by - ct)$, and

(b) Similarity solutions: $S = t^q f(xt^\gamma, yt^\gamma)$. Although both will produce solutions, through coupled ordinary differential equations, there is no hope of satisfying realistic boundary conditions. Neither was pursued.

[2] Uncoupled solutions found by the following steps:

(a) Guess a velocity field (the least sensitive to changes at the front), that must be rotational with source/sink at corners.

(b) Given $(u, v) = -\lambda(S)\nabla p$, find S from $S_t = \nabla \cdot (f(S)\vec{v}) = 0$ and then find p. This approach turned out to be more difficult than originally estimated and was not pursued.

[3] Assume the flow is radially symmetric:

(a) This is the same as the *local* flow around a source. This was the approach that was considered in detail and in the next section we elaborate on this case. This approach has been considered before. For example, Bajor et al. [1] test the grid orientation problem on a radially symmetric problem, although their paper omits any details of the analytic solution. So far the exact radially symmetric solution has not been located in the literature.

An attempt was also made to check the solution with a simple numerical code. John Stockie had a code available from an undergraduate project. [It turned out that this code, from Waterloo, was originally developed in part by Peter Sammon.] This code is unlikely to produce anything new in a short time but could be useful as a check.

3.6 Radially Symmetric Flow

The equations governing the pressure p and water saturation S are:

$$\nabla \cdot (\lambda(S)\nabla p) = 0, \text{ and } \phi S_t = \nabla \cdot (f(S)\lambda(S)\nabla p). \tag{6.6}$$

Assuming p and S are only functions of the radial variable r, these equations become

$$(r\lambda p_r)_r = 0, \text{ and } \phi S_t = \frac{1}{r}(rf(S)\lambda(S)p_r)_r. \tag{6.7}$$

We consider a source at $r = a$ of finite size, then from equation (6.9)

$$a\lambda(S)p_r = -g(t), \tag{6.8}$$

where $g(t)$ is an arbitrary source function. The negative sign indicates that $p_r < 0$ for outflow. From this, we obtain

$$\frac{\phi}{g(t)}S_t = -\frac{1}{r}[f(S)]_r. \tag{6.9}$$

Defining the new time variable τ as

$$\tau = \int_0^t \frac{g(\bar{t})}{\phi} d\bar{t}, \tag{6.10}$$

in terms of τ, (6.9) becomes

$$S_\tau + \frac{1}{r}[f(S)]_r = 0. \tag{6.11}$$

Redefining the source as $g(t) \equiv G(\tau)$ the initial and boundary conditions are:

$$S = \begin{cases} G(\tau) & r = a, \tau \geq 0 \\ 0 & r \succ a, \tau = 0. \end{cases} \tag{6.12}$$

Many different solutions to the problem arise, depending on the behaviour of the fractional flow function $f(S)$ and the initial function $G(\tau)$. We will usually consider $G(\tau)$ as a step function, so will concentrate on various forms of $f(S)$. For convenience, from now on we set $\tau = t$.

Case 1. If $f(S)$ is convex ($f''(S) > 0$), then

$$S = \begin{cases} G(\alpha) & \left(t \geq \dfrac{r^2 - a^2}{2f'(G(0))}\right) \\ 0 & \left(t < \dfrac{r^2 - a^2}{2f'(G(0))}\right). \end{cases} \tag{6.13}$$

The characteristic variable, α, is defined by

$$t - \alpha = \frac{r^2 - a^2}{2f'(G(\alpha))}, \tag{6.14}$$

so that $t = \alpha$ at $r = a$.

In this case, we have a simple solution along characteristics. A shock occurs if

$$f''(G)G'(\alpha) = f'(G), \tag{6.15}$$

and therefore depends on f and G. For example, an $f = G^2$ shock occurs if $G'(\alpha) = G(\alpha)$ for some α.

If $r = U(t)$ is the shock path, it is determined by the shock condition:

$$\frac{dU}{dt} = \frac{f^+ - f^-}{(S^+ - S^-)U} \tag{6.16}$$

When $G(\alpha)$ is a step function, a single shock appears in plots of the saturation S as a function of radial distance r from the source. The shock propagates in the positive r direction as time increases. This case would provide a good numerical test for non-smearing and grid dependencies. The shock path is given by

$$U^2 - a^2 = 2t(f(1) - f(0)). \tag{6.17}$$

Case 2. When $f(S)$ is concave there is no shock for the same step function input. The solution is smooth, corresponding to a rarefaction wave connecting the characteristics carrying $S = 1$ and $S = 0$.

Case 3. The best test of all is for the real f. For example, f is convex for $0 < S < L$ and concave for $L < S < 1$. Here, $f'(L) = f(L)/L$ and $f'(1) \neq 0$. The general form of the solution for the water saturation is

$$\text{Constant } (S = 1) \mid \text{Rarefraction } (S = Q) \mid \text{Shock} \mid \text{Constant } (S = 0). \tag{6.18}$$

The characteristic net is divided into three regions with the corresponding solutions:

$$S = \begin{cases} 1 & \left(t \geq \dfrac{r^2 - a^2}{2f'(1)}\right) \\ N & \left(\dfrac{r^2 - a^2}{2f'(1)} \leq t \leq \dfrac{r^2 - a^2}{2f'(L)}\right) \\ 0 & \left(t < \dfrac{r^2 - a^2}{2f'(L)}\right), \end{cases} \tag{6.19}$$

where N is given by

$$L \leq N \leq 1;\ f'(N) = Q$$
$$Q = (r^2 - a^2)/2t,\ f'(1) \leq Q \leq f'(L).$$

This case tests both the smooth parts of the flow *and* shock-smearing. Figure 3.4 displays the characteristic curves for the mixed convex/concave f case.

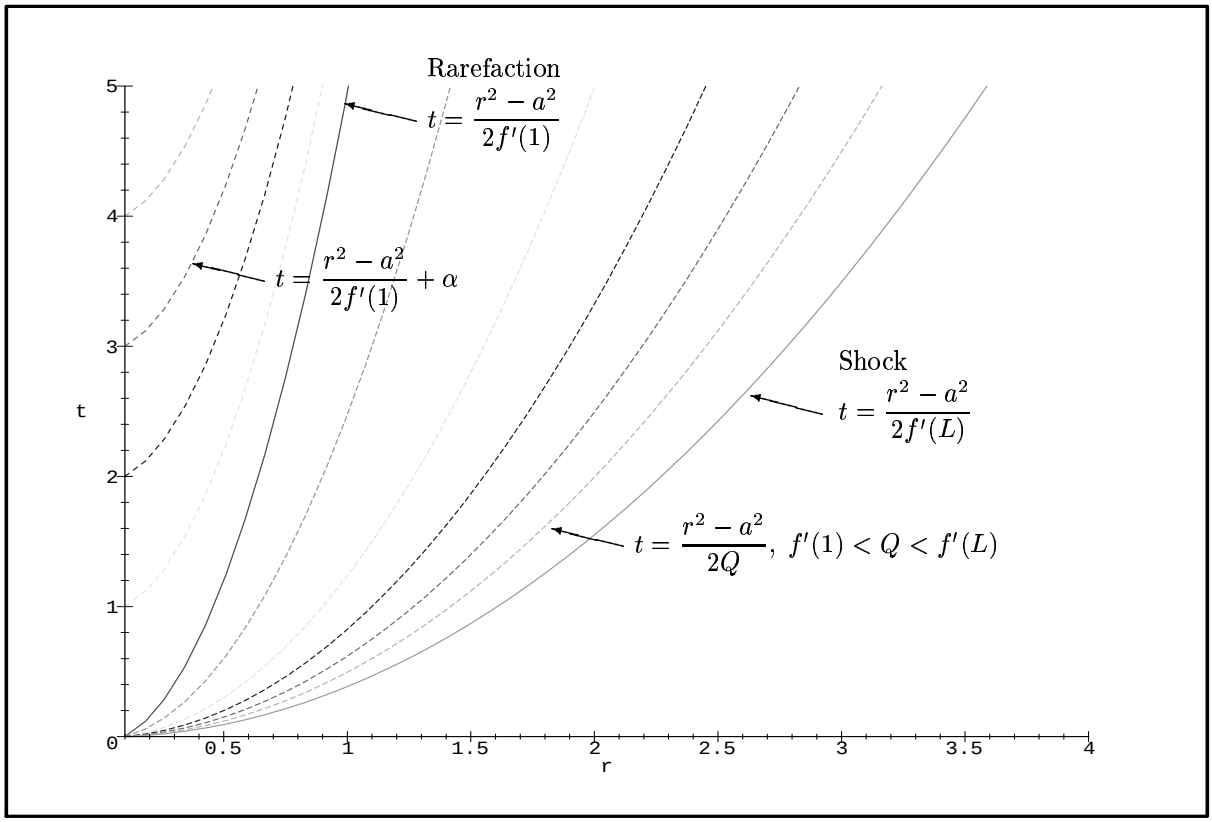

Figure 3.4: Characteristic curves for the mixed convex/concave f case.

3.7 Results and Discussion

We present the results of our study through various examples.

For $M = 10$, $\alpha = 4$ and $\beta = 1$, we have plotted the saturation profile in Figure 3.5 and the pressure profile in Figure 3.6 for two fixed times.

We computed the pressure and saturation solutions using a simple numerical code (implicit in pressure and explicit in saturation). Figures 3.7 and 3.8 display the resulting pressure and saturation fields along a ray emanating from the injector (source) to the producer (sink). Figures 3.9 and 3.10 show the corresponding pressure and saturation fields over the entire solution domain.

3.8 Stability and Well-posedness

Although we are confident that the radially symmetric problem described above should provide a good test for both shock-capturing and grid orientation dependence, it is worth expending some thought on the question of whether or not the generic flow problem is well-posed or not. To begin to understand why we might anticipate difficulties, we consider first the standard porous medium problem. This exhibits similarities to the full oil recovery problem considered above, but is technically much simpler.

Assume that the region to the left of the boundary $f(x, y, t) = 0$ (see Figure 3.11 for schematic details) is a porous medium filled with fluid, whilst to the right there is no fluid. By Darcy's law we

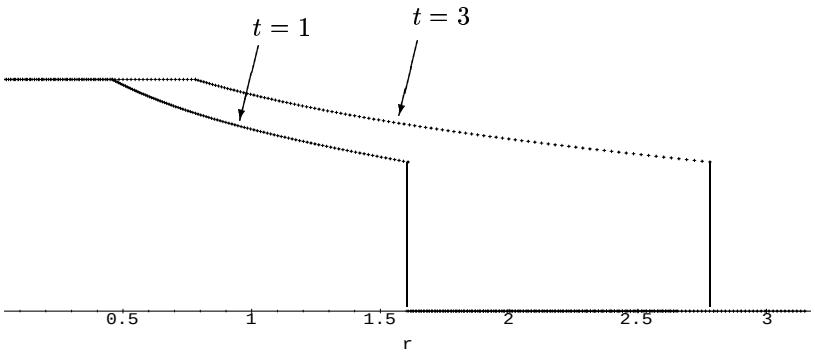

Figure 3.5: Saturation S versus radial variable r at times $t = 1$ and $t = 3$ for $M = 10$, $\alpha = 4$ and $\beta = 1$.

have

$$\boldsymbol{q} = -k\nabla p$$

where, as usual, $\boldsymbol{q}$ and p denote the velocity and pressure respectively and k (dimensions msec/kg) is the relative permeability. For incompressible fluid, conservation of mass now gives the equation of motion in the fluid-filled porous medium as

$$\nabla^2 p = 0.$$

As far as boundary conditions are concerned, we assume that the pressure is given on $f = 0$ by $p = p_a$, say. Another condition is also needed to determine the free boundary; this condition simply asserts that $Df/Dt = 0$ on $f = 0$ where D/Dt denotes the Lagrangean derivative. We find that, on $f = 0$, we must have

$$f_t = k\nabla p \cdot \nabla f.$$

This problem has a simple traveling wave solution with speed v; it is given by

$$p = p_a + \frac{v}{k}(vt - x), \qquad f = x - vt.$$

We wish to determine under what circumstances this traveling wave is stable to y-perturbations. Proceeding in the obvious fashion, we consider linear stability by assuming that

$$\begin{aligned} p &= p_a + \frac{v}{k}(vt - x) + \epsilon g(x,t)\sin ny \\ f &= x - vt + \epsilon e^{qt}\sin ny \end{aligned}$$

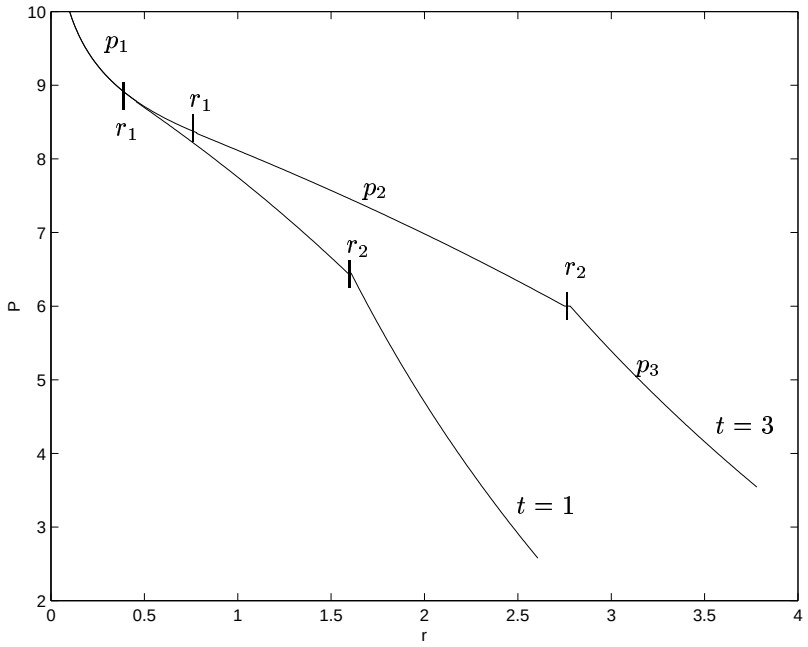

Figure 3.6: Pressure p versus radial variable r at times $t = 1$ and $t = 3$ for $M = 10$, $\alpha = 4$ and $\beta = 1$. For $a < r \leq r_1$, $p = p_1 = p_a - (A/\lambda(1))\ln(r/a)$. For $r_1 \leq r \leq r_2$, $p = p_2 = p_1(r_1) - A\int_{r_1}^{r}(1/\lambda(S(a))q)dq$. For $r > r_2$, $p = p_3 = p_3(r_2) - (A/\lambda(0))\ln(r/r_2)$.

where $\epsilon \ll 1$ and $g(x,t)$ and the amplification factor q are to be determined. The flow equation in the fluid-filled porous medium gives

$$g = A(t)e^{nx} + B(t)e^{-nx}$$

and assuming without loss of generality that $n > 0$, we must take $B = 0$ so that the perturbations become negligible as $x \to -\infty$. Imposing $p = p_a$ and $f_t = k\nabla p \cdot \nabla f$ on $x = vt - \epsilon e^{qt}\sin ny$ now gives the equations

$$\begin{aligned} 0 &= \frac{v}{k}e^{qt} + A(t)e^{nvt}, \\ \frac{q}{k}e^{qt} &= nA(t)e^{nvt} \end{aligned}$$

so that $q = -vn$ and $A(t) = (-v/k)\exp(-2nvt)$. Since n was assumed to be greater than zero, we recover the well-known result that *retreating* flow ($v < 0$) in a porous medium is unstable. (A very similar argument may be applied to the Hele-Shaw flow shown in Figure 3.12 to show that retreating fronts in such a cell are unstable.)

This result is potentially worrying. If we consider a retreating porous medium flow as discussed above as one where a 'more viscous' fluid (water) is being expelled by a 'less viscous' fluid (air), which is the case that pertains for nearly all of CMG's calculations, then the instability of the process could lead to gross errors in the numerical calculations. To be sure that this problem is present, however, we need to ensure that instability is present for the full equations.

3.8.1 Stability of a Paradigm Shock Solution

In this subsection we analyze a simple paradigm shock problem to finish developing the methodology necessary to attack the full problem.

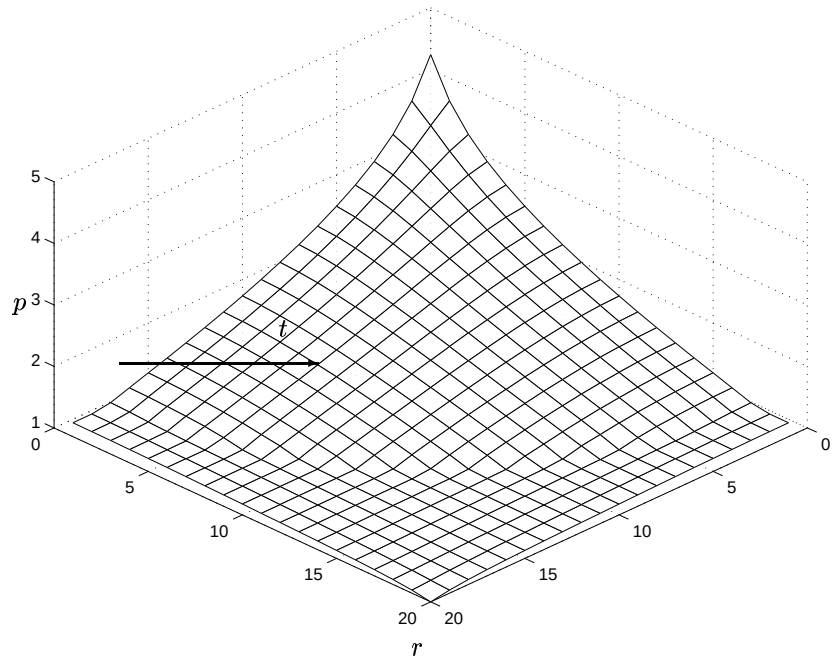

Figure 3.7: Pressure field p along a ray emanating from the injector to the producer (computed using the simple numerical code).

To illustrate the methods that we wish to use, consider the conservation law

$$S_t + (S^2/2)_x + (S^2/2)_y = 0.$$

It is easily confirmed that this possesses the one-dimensional shock solution

$$S = \begin{cases} S_L & (x < vt) \\ 0 & (x \geq vt) \end{cases}$$

where, according to the standard jump condition with $f(S) = S^2/2$

$$v = \frac{[f(S)]}{[S]} = \frac{S_L}{2}.$$

We note also that since $f'(S_L) = S_L$ and $f'(S_R) = 0$ then the entropy condition $f'(S_L) > v > f'(S_R)$ is satisfied and so according to the standard theorems (see, for example Smoller [5]) the solution that has been determined is unique.

We now wish to examine the stability of this solution. Using the *ansatz* that, for a perturbed shock,

$$\begin{aligned} \psi &= x - vt - \epsilon f(y,t) \\ S &= S_L + \epsilon g(y,t) \qquad \text{(left of the shock)} \\ S &= 0 + \epsilon h(y,t) \qquad \text{(right of the shock)} \end{aligned}$$

we find that h and g satisfy the partial differential equations

$$g_t + S_L(g_x + g_y) = 0, \qquad h_t = 0$$

whilst the jump condition (evaluated at the perturbed shock front) gives at $\mathrm{O}(\epsilon)$

$$-S_L f_t - v\tilde{g} + v\tilde{h} + S_L\tilde{g} - \frac{1}{2}S_L^2 f_y$$

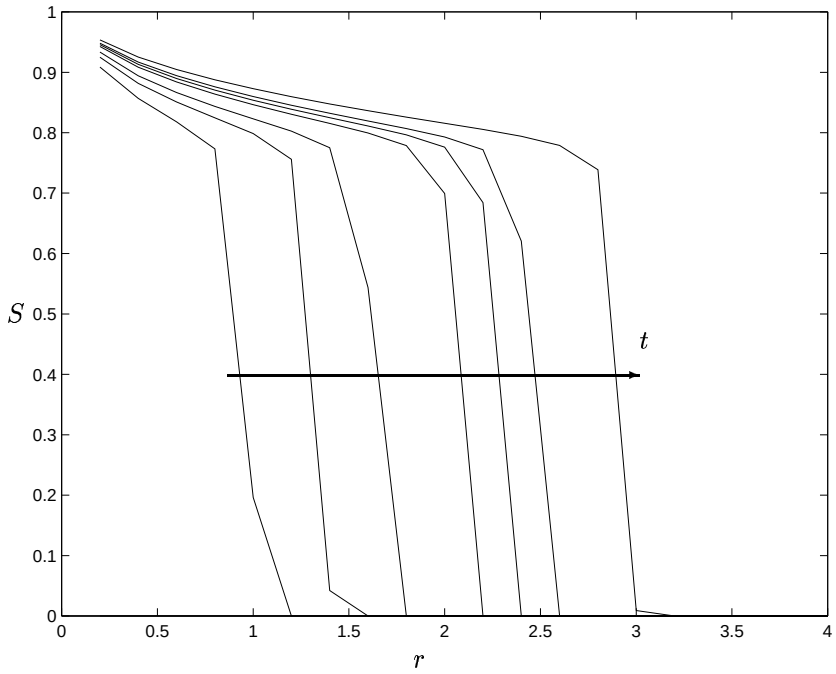

Figure 3.8: Saturation field S along a ray emanating from the injector to the producer (computed using the simple numerical code).

where $\tilde{g} = g(vt, y, t)$, $\tilde{h} = h(vt, y, t)$. Now suppose that the perturbation is of the obvious form

$$f(y,t) = Re(e^{iny}e^{\sigma t}).$$

Then the equations rapidly give $h = 0$ and $g = g_1(x)e^{iny}e^{\sigma t}$, followed by $g_1(x) = 2\sigma + inS_L$ and $\sigma = -iS_L n$. Thus the shock is neutrally stable (applied perturbations neither grow nor decay) and, on taking real parts,

$$\begin{aligned} \psi &= x - \frac{S_L}{2}t - \epsilon\cos(n(y - S_L t)) \\ S &= S_L + \epsilon n S_L \sin(n(y - S_L t)) \qquad \text{(left of the shock)} \\ S &= 0 \qquad \text{(right of the shock).} \end{aligned}$$

3.8.2 Stability for the Oil recovery problem

Guided by the methodology of the previous two subsections, we now consider the stability of the problem

$$(\lambda(S)p_x)_x + (\lambda(S)p_y)_y = 0 \tag{8.1}$$

$$(f(S)\lambda(S)p_x)_x + (f(S)\lambda(S)p_y)_y = S_t, \tag{8.2}$$

Here we have assumed without loss of generality that $\phi = 1$. For simplicity we consider the case $\alpha = \beta = 1$ (see later remarks) so that

$$f(S) = \frac{S}{S + \frac{1-S}{M}}, \qquad \lambda(S) = \frac{k}{\mu_w}\left(\frac{1-S}{M} + S\right).$$

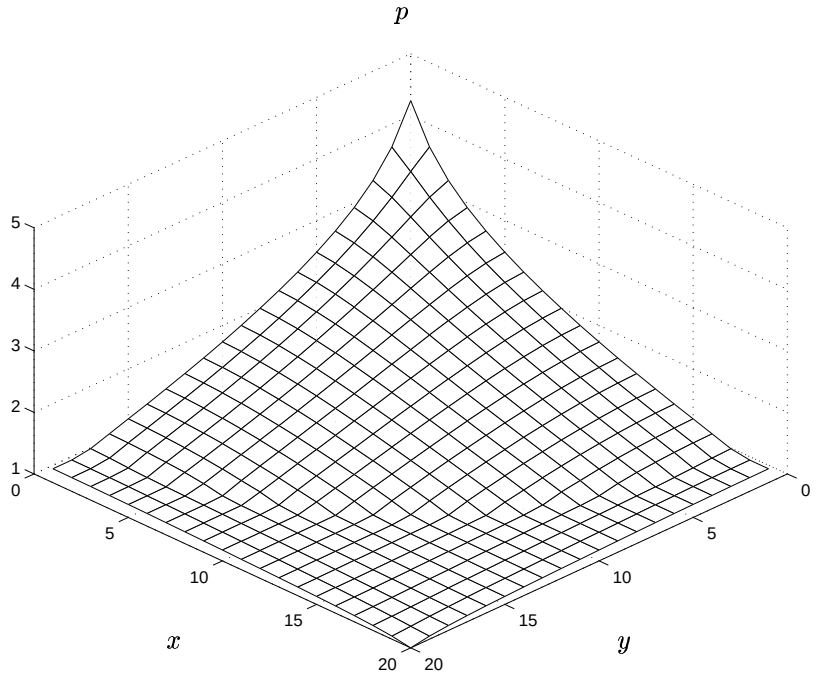

Figure 3.9: Pressure field p in the entire solution domain (computed using the simple numerical code).

Perturbing the problem in a similar fashion to the previous subsection, we assume that

$$\psi = x - t - \epsilon e^{\sigma t} e^{iny} + O(\epsilon^2) \tag{8.3}$$

$$S_L = 1 - \epsilon a(x,y,t) + O(\epsilon^2) \tag{8.4}$$

$$S_R = \epsilon b(x,y,t) + O(\epsilon^2) \tag{8.5}$$

$$p_L = -\frac{\mu_w x}{k} + \frac{t}{k}(\mu_w - \mu_o) + \epsilon c(x,y,t) + O(\epsilon^2) \tag{8.6}$$

$$p_R = -\frac{\mu_o x}{k} + \epsilon d(x,y,t) + O(\epsilon^2) \tag{8.7}$$

where by convention real parts are taken throughout. Note that the form of this *ansatz* ensures (a) that the pressure is continuous to leading order at the shock front, (b) that the one-dimensional solution is a shock of amplitude 1, and so by the jump conditions the shock speed is one, and (c) in the one-dimensional solution $\lambda p_x = -1$, so that the flux of material is constant in time and the front moves from left to right. (Fluxes that are functions of time may easily be dealt with by rescaling time as described above.)

We now need to pick a, b, c, d and σ so that the following conditions are satisfied:

- s_L and p_L satisfy the partial differential equations (8.1) and (8.2) to the left of the shock.
- s_R and p_R satisfy the partial differential equations (8.1) and (8.2) to the right of the shock.
- The correct jump conditions for (8.1) and (8.2) are satisfied.
- The pressure is continuous to O(ϵ) at the shock front.

Courant & Hilbert [2] give the jump conditions for a system of k conservation laws in n independent variables. If the system is written in conservation form as

$$\sum_{i=1}^{n} \frac{\partial P_{ij}}{\partial x_i} = 0 \qquad (j = 1, 2, ..., k)$$

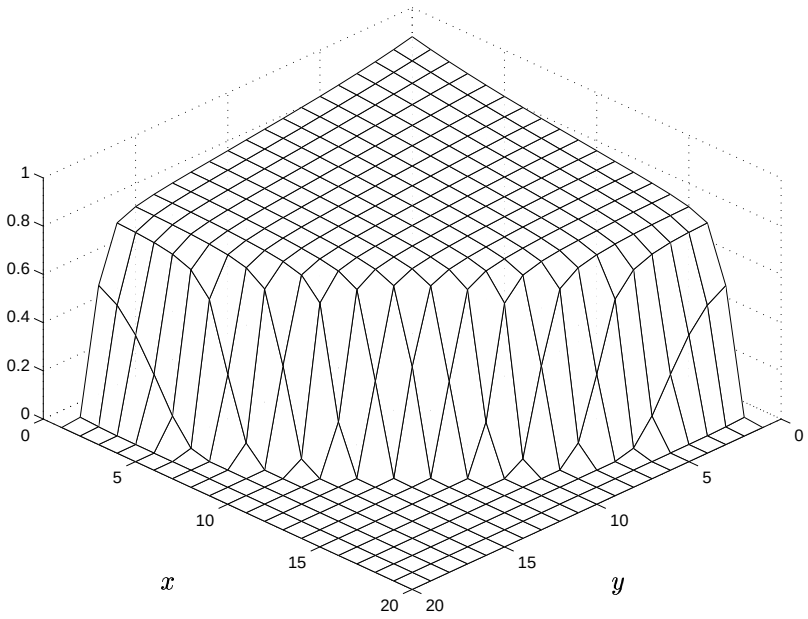

Figure 3.10: Saturation field S in the entire solution domain (computed using the simple numerical code).

some simple analysis shows that if the shock front is given by

$$\psi(x_1, x_2, ..., x_n) = 0$$

then the jump conditions are

$$\sum_{i=1}^{n} [P_{ij}] \frac{\partial \psi}{\partial x_i} \qquad (j = 1, 2, ..., k)$$

where, as usual, [.] denotes the jump in a quantity as the shock $\psi = 0$ is crossed. For the equations above the jump conditions are therefore

$$[\lambda p_x]\psi_x + [\lambda p_y]\psi_y = 0 \qquad [S]\psi_t - [f\lambda p_x]\psi_x - [f\lambda p_y]\psi_y = 0.$$

Inserting the *ansatz* into the relevant equations in the order indicated above, we find that at $O(\epsilon)$ the following seven equations must be satisfied:

$$c_{xx} + c_{yy} + \frac{\mu_w}{Mk}(M-1)a_x = 0 \tag{8.8}$$

$$c_{xx} + c_{yy} + \frac{\mu_w}{k}(a_t + a_x) = 0 \tag{8.9}$$

$$d_{xx} + d_{yy} + \frac{\mu_o}{k}(1-M)b_x = 0 \tag{8.10}$$

$$b_t + Mb_x = 0 \tag{8.11}$$

$$c_x - \frac{1}{M}d_x + \frac{(1-M)}{Mk}[-a\mu_w - b\mu_o] = 0 \tag{8.12}$$

$$-\sigma e^{\sigma t} e^{iny} + b(1-M) - \frac{k}{\mu_w}c_x = 0 \tag{8.13}$$

$$\frac{\mu_o - \mu_w}{k} e^{\sigma t} e^{iny} + c - d = 0 \tag{8.14}$$

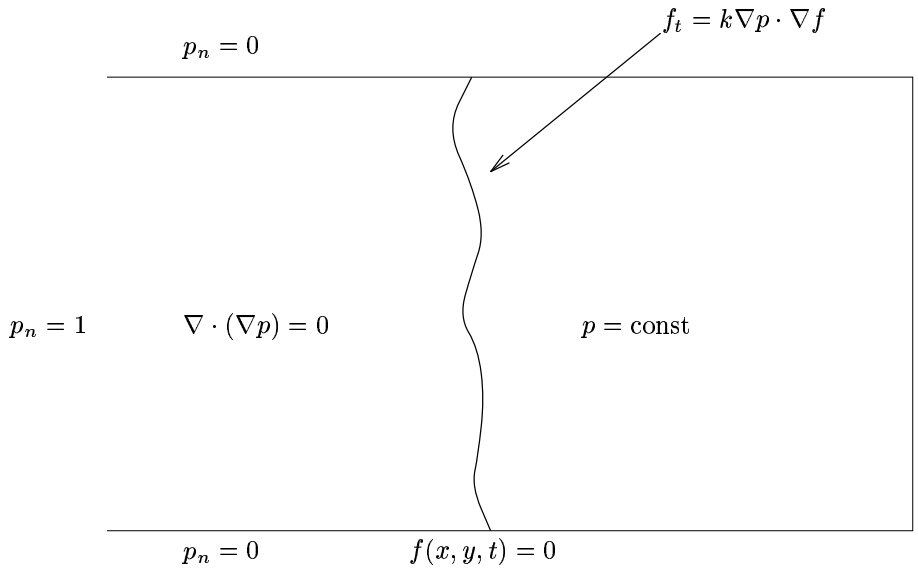

Figure 3.11: Darcy porous medium.

The first four of these equations are partial differential equations for functions of x, y and t, whilst the last three are to be evaluated at $x = t$ and are therefore equations in the independent variables y and t only.

To solve (8.8)-(8.14), we make the further *ansatz* (again assuming that real parts are taken throughout) that

$$a = a_1 e^{a_2(Mx-t)} e^{iny} \tag{8.15}$$
$$b = b_1 e^{b_2(x-Mt)} e^{iny} \tag{8.16}$$
$$c = c_1 e^{a_2(Mx-t)} e^{iny} \tag{8.17}$$
$$d = d_1 e^{b_2(x-Mt)} e^{iny}, \tag{8.18}$$

these choices having been made so as to automatically satisfy (8.11) and the simple equation that results from subtracting (8.9) from (8.8). Now (8.13) gives the three equations

$$b_2(1-M) = \sigma \tag{8.19}$$
$$a_2(M-1) = \sigma \tag{8.20}$$
$$(1-M)b_1 - \frac{k}{\mu_w} M a_2 c_1 = \sigma \tag{8.21}$$

whilst (8.8), (8.10), (8.12) and (8.14) in turn give

$$M^2 c_1 a_2^2 - n^2 c_1 + \frac{\mu_w}{k}(M-1)a_1 a_2 = 0 \tag{8.22}$$
$$d_1 b_2^2 - n^2 d_1 + \frac{\mu_o}{k}(1-M)b_1 b_2 = 0 \tag{8.23}$$
$$M c_1 a_2 - \frac{1}{M} b_2 d_1 + \frac{(1-M)}{Mk}[-\mu_w a_1 - \mu_o b_1] = 0 \tag{8.24}$$
$$c_1 - d_1 + \frac{\mu_o - \mu_w}{k} = 0. \tag{8.25}$$

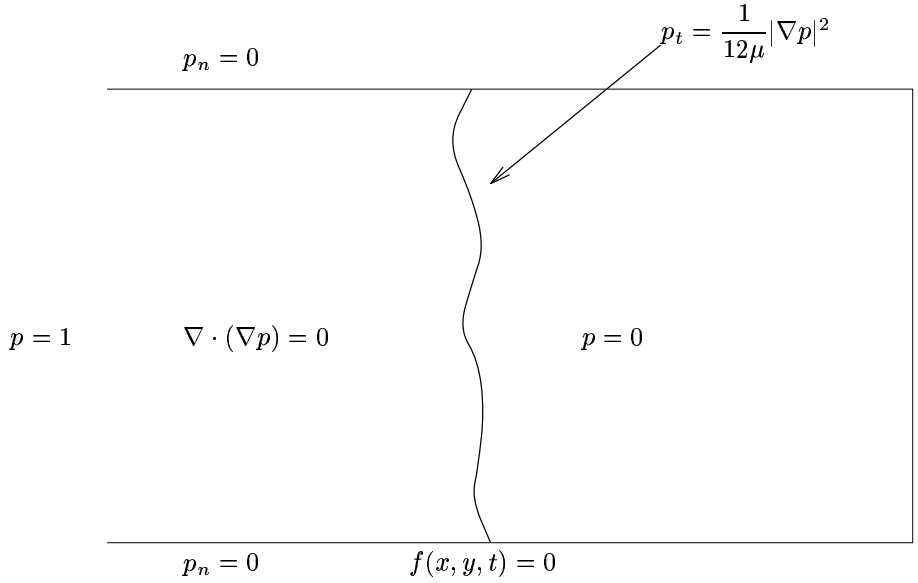

Figure 3.12: Hele-Shaw.

The equations (8.19)-(8.25) constitute seven equations in the seven unknowns a_1, b_1, c_1, d_1, a_2, b_2 and σ so nominally the problem formulation is complete.

Before proceeding further, let us consider how the *ansatz* that we have made is related to these equations. To the left of the shock, the perturbations must decay as $x \to -\infty$, so that necessarily $a_2 > 0$. But now if $\mu_o > \mu_w$ so that M exceeds 1 (as is normally the case), then (8.20) suggests that σ is positive. A similar argument applied to the right of the shock shows that $b_2 < 0$ and gives the same conclusion regarding the sign of σ. Thus according to (8.3) the shock position is unstable and perturbations grow exponentially. This instability is likely to manifest itself as 'fingering', where the water infiltrates the oil in an unstable manner, similar to the porous medium instability discussed above. As far as the size of the shock is concerned, we note from (8.15) that since $a_2 > 0$, perturbations to the left of the shock decay exponentially in time. To the right of the shock, however, since $b_2 < 0$ th perturbations grow exponentially. Thus both the position of the shock front and S are linearly unstable. (Since we have examined the case $\alpha = \beta = 1$ there is no technical reason why S cannot take values less than zero, which is unphysical. When α and β are not one, however, this problem may easily be dealt with.)

Although the conclusion that the simple shock front solution is unstable now seems unavoidable, it is necessary to check (for consistency) that amplification factors with positive real parts actually exist. Eliminating a_2, b_1, b_2 and d_1 we find from (8.22), (8.23) and (8.24) that

$$c_1 \left(\frac{\sigma^2 M^2}{(M-1)^2} - n^2 \right) + \frac{\mu_w a_1 \sigma}{k} = 0$$

$$\left(c_1 + \frac{\mu_o - \mu_w}{k} \right) \left(\frac{\sigma^2}{(1-M)^2} - n^2 \right) + \frac{\mu_o \sigma^2}{k(1-M)} \left(1 + \frac{kMc_1}{\mu_w(M-1)} \right) = 0$$

$$\frac{c_1 M \sigma}{M-1} + \frac{\sigma}{M(M-1)} \left(c_1 + \frac{\mu_o - \mu_w}{k} \right) +$$

$$\frac{(1-M)}{kM}\left(-a_1\mu_w - \frac{\mu_o}{1-M}\left(\sigma + \frac{k\sigma M c_1}{\mu_w(1-M)}\right)\right) = 0$$

and a_1 and c_1 may now be eliminated to give an equation involving σ alone. After some (rather tedious and lengthy) calculations, we find that the amplification rate σ satisfies the quintic equation $\theta(\sigma) = 0$ where

$$\theta(\sigma) = K\sigma^5 + M(1-M)^2\sigma^4 - Kn^2(1-M)\sigma^3 - n^2M^2(1-M)^3\sigma^2 + n^4(1-M)^5 \qquad (8.26)$$

and $K = k/\mu_w$. This equation is tedious to analyze (though various special cases where the parameters K, M and n are large or small may be examined), but we note immediately that $\theta(0) < 0$ for $M > 1$ whilst for $\theta(\sigma) \to +\infty$ as $\sigma \to +\infty$. It is therefore certain that a real root greater than zero exists, confirming that the problem as posed is, indeed, ill-posed.

What may we conclude from this analysis? Unfortunately it seems clear that, as might be expected, the simple porous medium result that forcing a more viscous fluid with a less viscous one is unstable is not altered for the more complicated oil recovery problem. This is likely to lead to difficulties in computing numerical results, and may be one of the factors that influences the grid orientation dependence. As far as the computation of numerical results is concerned, of course, the code is unlikely to 'see' the equations (8.1) and (8.2). Instead, the discretization used will introduce 'artificial' viscosity and other dissipative mechanisms which may act to at least partially damp out numerical instabilities.

Finally, a few general comments are in order. Although for simplicity we only considered the case $\alpha = \beta = 1$ in detail, other values of α and β may be dealt by making various changes to the solution *ansatz*. We have not analyzed these fully yet, but it seems likely that the conclusions will be similar. We also note that, whilst the first two problems analyzed in this section are standard book work, we have not been able to find an analysis of shock front stability for the full oil recovery problem in the literature, though it seems likely that one must exist somewhere.

Acknowledgment

We would like to thank Peter Sammon for explaining the petroleum reservoir simulation problem to us and for answering our constant deluge of questions.

3.9 References

[1] Bajor and Cormack, The Quantitative Characterisation of the Grid Orientation Problem, AOSTRA of Research, Vo. 235, 1992.

[2] R. Courant and D. Hilbert, Methods of Mathematical Physics, Wiley-Interscience, Vol. 2, New York, 1962.

[3] T.A. McCracken and J L. Yanosik, A nine-point, finite difference reservoir simulator for realistic prediction of adverse mobility ratio displacements, Transactions AIME, Vol. 267, 1979, pp. 253–262.

[4] M.K. Abdou et. al., Impact of grid selection on reservoir simulation, Journal of Petroleum Technology, Vol. 45, 1993, pp. 664–669.

[5] J. Smoller, Shock Waves and Reaction-Diffusion Equations, Springer-Verlag, 1983.